

**OPTICAL EXPERIMENTAL METHODS APPLIED IN THE INVESTIGATION OF THE
ORTHOTROPIC AND ANISOTROPIC MATERIALS AND STRUCTURES**

Ioan SZÁVA

Prof.dr.eng. - TRANSILVANIA University in Brasov – Faculty of Mechanical Engineering

Address: B-dul Eroilor nr. 29, 50036 Brasov, Romania

E-mail: janoska@clicknet.ro

Botond-Pál GÁLFI

Dr.eng. – TRANSILVANIA University in Brasov – Faculty of Mechanical Engineering

Address: B-dul Eroilor nr. 29, 50036 Brasov, Romania

E-mail: bgalfi@yahoo.com

Abstract:

The experimental approach of the orthotropic and anisotropic materials requires special investigation methods. Due to their mechanical properties, which depend strongly on the direction of the investigation, several classical experimental methods cannot be applied efficiently. The authors offer an over-view of the most efficiently methods in this sense, which were applied by them during the last period not only on the wood-, and wood-based materials, but also on different types of composite materials, too. The described testing devices and approaches are originals, and the obtained results can be useful for those scientists, who are interested in further high-accuracy experimental investigations of the stress-strain states of these kinds of materials or/and structures.

Key words: *orthotropic and anisotropic material; strain-state; optical full-field non-contact methods.*

INTRODUCTION

The wood-, and wood-based materials present special requirements from the point of view of the experimental investigations. In this sense, a high-accuracy evaluation of their stress-, respectively strain-state require such experimental methods, which are able putting in evidence the stress/or strain values along different directions on the specimens surfaces. Based on these values, became possible to obtaining the requested main values of the stresses or of the strains. Basically, one can be applied successfully only the so-called "*full-field methods*" (PhotoStress - the Thin Layer Photo-elastic Coatings, Moiré-Fringe, Holographic Interferometry, ESPI (Electronique Speckle Pattern Interferometry), respectively Video Image Correlation (VIC) methods. The last one is also known as Digital Image Correlation (DIC) method, too. The so-called "*local experimental methods*", like Electric Strain Gauges, aren't enough efficiently, because they offer information only in a point and along one well-defined direction. The authors, during several years, applied the above-mentioned full-field methods. In this contribution they try proving their efficiency in the wood-based materials and structures investigations.

Also, in the literature there are a significant number of studies, briefly presented in the following.

The authors of the paper (Niemz 2012) offer a comprehensive overview of the NDT methods applied in the monitoring of the cultural heritage wood structures and their elements. Taking into the consideration the topics of the present paper, one can put in evidence several important aspects, analyzed briefly subsequently. In order to evaluate the strain-stress states, respectively to establish the mechanical characteristics (Young moduli, Poisson's ratios etc.) are presented the Electric Strain Gauge-, respectively the Video Image Correlation methods, with some interesting and useful results. These methods are also suitable for moisture-induced effects evaluation (e.g. distortion, stress etc.) and they are widely applied in wood industry. By means of Acoustic Emission method, described also in the same contribution, became possible to monitor the health-state of the analyzed wood members. An other useful method, the evaluation of the sound waves speed, offers practical information on the magnitude of the different kind of moduli of elasticity. Several other interesting and useful investigation methods are described by the authors (e.g. X-Ray Computer Tomography, NIR-spectroscopy, Thermography etc.), in order to obtain more complex information on the wood-members health-states.

In reference (Bucur 2006) is shown, that at least three longitudinal and three shear wave velocities propagating along the principal axes of anisotropy, and additionally, three quasi-shear wave velocities measured at a suitable angle with respect to the principal axes of anisotropy are needed in order to determine all independent components of the stiffness matrix. This remark was applied in the reference (Ozyhar *et al.* 2013e), where the authors investigated the influence of moisture content on the elastic characteristics of beech wood (*Fagus sylvatica* L.) by means of ultrasonic waves. A set of elastic engineering parameters (i.e. three Young's moduli, three shear moduli and six Poisson's ratios) is determined at four specific moisture contents. The results reveal the significant influence of the moisture content on the elastic behaviour of beech wood. The authors proved by their experimental results, that with the exception of some Poisson's ratios, the engineering parameters decrease with increasing moisture content, indicating a decline in stiffness at higher moisture contents. At the same time, wood anisotropy, displayed by the two-dimensional representation of the velocity surface, remains almost unchanged. The results prove that the ultrasonic technique is suitable for determining the elastic moduli. However, non-diagonal terms of the stiffness matrix must be considered when calculating the Young's moduli. This is shown experimentally by comparing the ultrasonic Young's moduli calculated without, and allowing for, the non-diagonal terms. While the ultrasonic technique is found to be reliable to measure the elastic moduli (based on the measured values), its eligibility to measure the Poisson's ratios remains uncertain. The authors used the direct pulse transmission ultrasonic technique in order to obtaining the wave velocities.

How the authors of the reference (Ozyhar *et al.* 2012a) stated in their contribution, while the general mechanical behaviour of wood is known, its moisture-dependent elastic and strength anisotropy remains little studied. Given the anisotropic and hygroscopic nature of wood, a characterization of wood mechanical behaviour will require knowledge of its moisture-dependent properties in relation to the three principal axes of anisotropy. Consequently, the authors examine the influence of the moisture content (MC) on the elastic and strength anisotropy of beech wood (*Fagus sylvatica* L.). Selected elastic and strength parameters, including the anisotropic Young's moduli, Poisson's ratios, yield and ultimate stress values and the fracture toughness in the **TR**, **TL**, **RT** and **RL** directions, are determined in uni-axial tension and compact tension tests at different moisture conditions. A distinct moisture dependency is shown for the elastic and strength behaviour of beech wood. With the exception of some Poisson's ratios, all investigated elastic and strength parameters are shown to decrease with increasing MC. Three different specimen types, one for the measurement of the tensile properties in the **L** direction, a second one for the determination of the tensile properties in the **R** and **T** directions and a third one for the measurement of the fracture properties in tension, were needed to investigate the mechanical properties examined in this study.

The authors of the reference (Ozyhar *et al.* 2012b) present a significant part of their bigger research project devoted to the investigation of anisotropic moisture-dependent elastic and strength properties of

beech wood. The objective of this research was to determine the mechanical behaviour of European beech wood at high moisture levels. Therefore, investigations of the tensile, compressive and bending properties at different moisture levels near, and above the fibre saturation point (FSP) were conducted. Elastic and strength parameters, including Young's moduli and strength values, were determined with respect to the three axes of anisotropy (longitudinal, radial, tangential). The results demonstrate the significant influence of moisture content (MC) on the mechanical behaviour of beech wood. They show that Young's moduli and strength parameters decrease with increasing MC, whereby individual moduli and strength values are affected by the MC to different degrees. The experimental results further indicate that tensile, bending and compressive properties, in general, reach their minimum value near the FSP, even though, an increasing tendency was reported for the tensile and compressive Young's moduli and a decreasing trend for the tensile strength at MC higher than FSP. Since the effect on the mechanical properties caused by the increase in MC above the FSP is relatively small compared with that below the FSP, the changes in mechanical behaviour induced by MC variations above the FSP are found to be rather weak.

The authors of the reference (Ozyhar *et al.* 2013d) analyzed the influence of moisture content (MC) on the tension-compression asymmetry of beech wood. The elastic and strength parameters, including the tension and compression Young's moduli, Poisson's ratios, and ultimate and yield stress values, were determined and compared in terms of different moisture contents for all orthotropic directions. The results reveal a distinctive tension-compression strength asymmetry with a moisture dependency that is visualized clearly by the tension to compression yield stress ratio. The tension-compression asymmetry is further shown by the inequality of the elastic properties, known as the "bi-modular behavior". The latter is proven for the Young's moduli values in the radial and tangential directions and for individual Poisson's ratios. Although the bi-modularity of the Young's moduli is significant at low moisture content levels, there is no evidence of moisture dependency on the tension-compression asymmetry of the Poisson's ratios. A digital image correlation technique was used to capture the strains during deformation. The surface strains were calculated from the displacements that occurred during deformation using the VIC 2D soft-ware (Correlated Solution).

In the reference (Ozyhar *et al.* 2013c) the authors offer their comprehensive study on the visco-elastic behaviour of the wood. The time dependency of the orthotropic compliance for beech wood was investigated by performing tensile and compressive creep experiments in all wood's orthotropic directions. Time evolution of the creep strain in the axial and lateral directions were recorded using the digital image correlation technique, to determine the time dependent Young's moduli and the Poisson's ratios needed for the calculation of the diagonal and non-diagonal elements of the visco-elastic compliance matrix. The results of this study demonstrate the visco-elastic character of wood, revealing the significant time influence on the mechanical behavior. The unequal time dependency of the Young's moduli and the Poisson's ratios obtained for the individual directions highlights the orthotropic nature of the visco-elastic compliance. Differences between the time dependent behaviours for the compliance determined in tensile and compressive tests further indicate that the visco-elastic behavior of wood depends on the loading modality. Supported by the unequal evolution of the tensile and compressive creep strain, the results suggest that the time dependent stress – strain relationship of wood is essentially different in tensile and compressive loadings. Poisson's ratio values, which are shown to increase with time in tensile test and decrease in compressive test, demonstrated this fact. The substantially different time dependency of the non-diagonal elements of the compliance matrix further emphasizes the complexity of the visco-elastic character of wood. Visualized by the time evolution of the corresponding non-diagonal elements ratio, differences between the tensile and compressive visco-elastic behaviour become particularly visible in the time dependency of the orthotropic compliance asymmetry. A dog-bone shaped specimen was chosen for the creep experiments. The cuboid profile in the cross section of the specimen allows for the simultaneous measurement of lateral strains in two separate directions and is suitable to determine two Poisson's ratios on one specimen. The applicability of this specimen to measure the elastic properties for wood, both in tensile and compressive tests, has been demonstrated by the authors. A digital image correlation (DIC) technique (Vic-2D, Correlated Solutions) was used to capture the strains during the creep experiments.

The authors of the reference (Niemz *et al.* 2007) analyzed the strain distribution in the cross section of wood-based materials (OSB, fiber boards, MDF) by means of the in-plane Moiré technique for different (four points) bending stress. For comparison, the strain of the outer fiber on the tensile and pressure side of the samples was measured simultaneously by using strain gauges. The authors remarked that no displacement of the neutral layer in direction of the tensile side, as can be seen on solid wood, was noticed, because of the tensile and compression strength, which are of the same level for these materials. Concerning the strain of the outer fiber, a very good correspondence was observed between Moiré technique and strain gauges ones. In the reference (Valla *et al.* 2010) the authors offer a comprehensive comparative study, regarding on the suitability of Electronic Speckle Pattern Interferometry (ESPI) and Digital Image Correlation (DIC) for the measurement of two-dimensional strain distribution on mechanically stressed wood specimens. Particular attention is dedicated to the basics of the individual techniques in order to discuss potential advantages and

disadvantages. The results of a model experiment with plywood show that the results delivered by both methods are very similar and of high quality. ESPI provides reasonably fast experimental set-up and data acquisition, and fast, straightforward post-processing. Compared to ESPI, the DIC is a more versatile method demanding skilled sample preparation, and post-processing may be time consuming. The authors performed their comparative study on a simple uni-axial tensile experiment. Therefore, measuring conditions that can be handled by both methods without a problem were chosen. Particular attention was dedicated to a well-founded assessment of relevant parameters such as spatial resolution and displacement accuracy with regard to the two techniques. Tensile shear specimens were manufactured out of plywood boards. The area of interest (AOI) on the tested specimen was 20x10mm, and the notches were sawn with a 3.2mm-thick circular saw and were cut into the plywood board to a depth of approximately 14.5mm. The specimens were strained in tension by means of a Zwick/Roell Z100 universal testing machine.

OBJECTIVES

In the present contribution there are analyzed three full-field different experimental methods, respectively are described several original experimental approaches of the wood-, and wood-based structures from their strain-state's point of view. Starting from the Moiré-Fringe method, where there is a low-accuracy evaluation of the displacements, respectively of the linear strains, there are presented the Holographic Interferometry, respectively the VIC methods with useful applications in wood-based materials and structures.

METHOD, MATERIALS AND EQUIPMENT

Moiré-Fringe Method

The superposing of two similar grating (having parallel, equal-spaced, opaque lines with constant width in transparent and opaque parts/lines), which are slight relatively displaced each to other, produces the so-called moiré fringes (Fig. 1). There are two main methods: The Geometric Moiré Fringe, respectively The Shadow Moiré Fringe one. The first is applied for the in-plane displacements evaluation, and the second is useful especially for the out-of-plane displacements monitoring. Due to the fact, that the authors analyzed the displacements fields of the disk-shape wood specimens, depending on the fibre orientation, the first method was involved. In the Geometric Moiré Fringes Method one of the grids, named reference grating (RG) is kept separately from the object (so, it will not suffers any changing in its initial geometry) and the other grid, named specimen grating (SG), will be fixed to the object's surface (so, it will suffers together with the object the same deformations). The pitch of the reference grating is noted p_2 and for the specimen grating (after its deformation): p_1 . By superposing these relatively displaced grids (due to translation or rotation), we will obtain two families of curves, named *moiré fringes*.

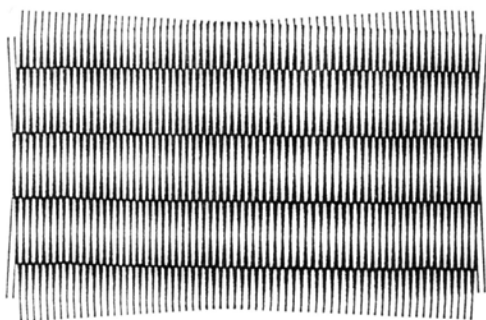


Fig. 1
Moiré fringes obtained by a small relative rotation of the grids.

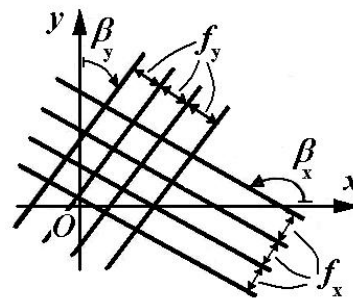


Fig. 2
Plane homogenous deformation.

In case of *the plane homogenous deformation* (Fig. 2), where $p_1 = p_2 = p$, the following relations between the fringe parameters and strain-state of the object are known:

$$\left. \begin{aligned} \varepsilon_x &= \frac{p}{f_x} \cdot \cos \beta_x; \\ \varepsilon_y &= \frac{p}{f_y} \cdot \cos \beta_y; \\ \gamma_{xy} &= \theta_x - \theta_y = \frac{p}{f_y} \cdot \sin \beta_y - \frac{p}{f_x} \cdot \sin \beta_x. \end{aligned} \right\} \quad (1)$$

In order to evaluate the in-plane displacements field of some disk-shape natural wood specimens, the authors conceived and realized an original device (Száva *et al.* 2007), shown in Fig. 3. In principle, a very rigid plate **6** is fixed on the fix member of the tensile testing machine and the second very rigid plate **1** is connected to the mobile member of the tensile testing machine. The disk-shaped wood specimen **4** is loaded with force **F** by means of the special shape components **3**. The applied force magnitude is monitored by means of the electric strain gauge force transducer **2**, and the total displacement of the disc (its diametrical contraction): with an original electric strain gauge lamella-shape displacement transducer **7**, fixed to plate **6** by means of the U-shape component **5**. The force transducer has a full- Wheatstone bridge connection, and the displacements transducer: a half-bridge one. By means of some adequate calibration, there are obtained the correspondence between the indicated mV and the real force, respectively displacement magnitudes.

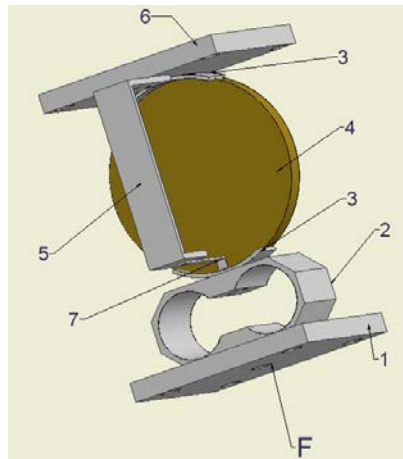


Fig. 3
The mono-directional testing device.

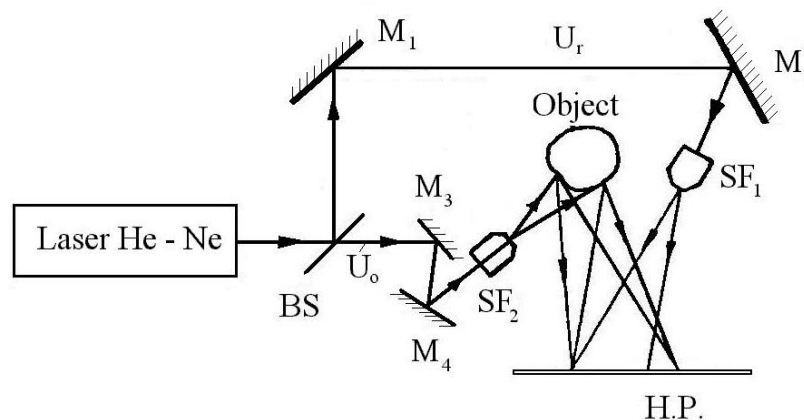


Fig. 4
The principle of transmission holograms.

Holographic Interferometry

The transmission holograms are used especially in technical activities (see Fig. 4). The monochromatic beam of light ray, emitted by a HeNe laser, is divided (by means of the beam splitter *BS*) in two parts: in a reflected part, named reference beam U_r and in a transmitted part, named object beam U_o . The reference beam has the following way: the mirrors M_1 , M_2 , the spatial filter SF_1 and the holographic plate *HP*. The object beam, by means of mirrors M_3 , M_4 and spatial filter SF_2 will arrive to the object. This spatial filter directs the light to the holographic plate, where it interferes with the reference beam. In this way, after a normal photo-processing, one obtains *the hologram* (a virtual 3D image of the tested object). If the exposure time is divided into two equal parts: first for the initial state of the object (for example unloaded one) and the second for the final state (the loaded one), then, after a normal photo processing and reconstruction, one can observe on the 3D virtual image of the object some fringes, named *interference fringes*. They are the result of the interference between the light scattered from two identical surfaces placed at slightly different positions in space (as result of the body' deformation, each point of the initial body/object will be slightly moved and will act as some secondary light sources, whom beams will interfere). These fringes represent for

engineers the most important information about the stress-strain state of the investigated object. One of the main advantage of the Holographic Interferometry consists of the fact, that it can be applied practically to all of materials (homogenous, or not, isotropic, orthotropic or anisotropic ones). A very important condition consists of a relatively low displacement field (less than $\lambda/4$, where λ represents the wavelength of the light); in case of HeNe lasers (red light), it is $\lambda=632.8nm$. One other limitation of the method consists of the very high-accuracy vibration-insulation of the system; consequently, in its common version it can be applied only in laboratory conditions, not in working ones.

In literature (Jones and Wykes 1983) is demonstrated that in general cases we need information from minimum 3 independent viewing directions in order to determine the whole components of the displacement in a point of the body (Fig. 5). For a simplified optical montage (Fig. 5), related in (Jones and Wykes 1983), one can simplify this calculus: it means that when the axes $x_1 O x_2 x_3$ are defined such that the object surface lies in the $x_2 x_3$ - plane, 9 coefficients must be calculated for each measurement in the three "general" viewing directions. In this case of described arrangement, the number of coefficients can be reduced from 27 to 13 and so, became possible a simplified fringe pattern evaluation. Other important simplification can be introduced in some particular cases (see the below-presented case), described in details in (Száva 2005).

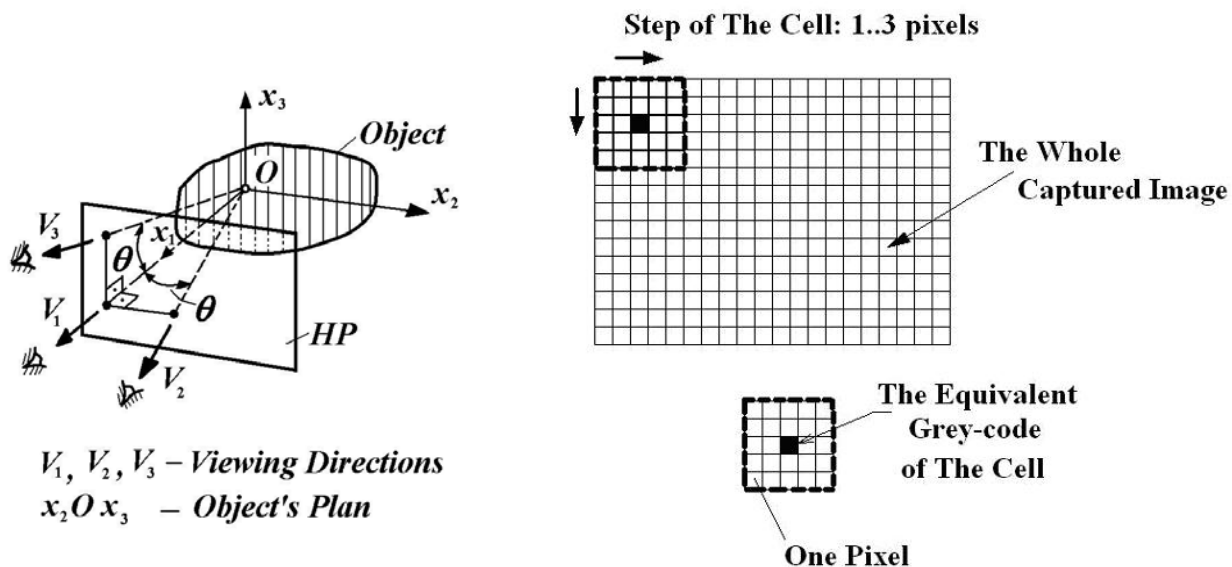


Fig. 5
The viewing positions for the displacements evaluation.

Fig. 6
The measuring principle based on the scanning procedure.

Video Image Correlation

In the described experimental investigation was used a *VIC System from ISI-Sys GmbH, Kassel, Germany*.

In principle, the system consists of two high-resolution video cameras, fixed on a very rigid Aluminium connection rod, mounted on a very stable tripod. The investigated object's surface is sprayed in advance with a water-soluble paint, in order to obtain a non-uniform dotted surface; the size of dots depends on the tested/investigated surface magnitude.

After a calibration, using some special targets, the cameras will perform the image acquisition in an $[n \cdot m]$ matrix of pixels, firstly for the unloaded specimen and later for the loaded one. On the unloaded specimen's images is defined *the Area of Interest*, respectively the proper *Subset* (see Fig. 6, where this Subset consists of a $5 \cdot 5 = 25$ pixels), respectively the optimal step-magnitude of the Subset, in order to be scanned/investigated the whole image by horizontal and vertical translation of it. For a nominal position of the Subset, the software will determine an unique grey-code, correlated to its median pixel's high-accuracy 3D coordinated. By analysing the whole captured image (corresponding to the unloaded state of the object), this will be substituted by means of these median pixels of the Subsets. A similarly analysis will be performed for each captured left-, and right images of the whole loading stages.

The software will compare the 3D displacements of these representative median pixels with their initial stage's ones and will draw-up the corresponding displacements vectors. Consequently, became possible to

follow, in 3D, not only the displacements, but also the corresponding strains of the significant points from the Area of Interest.

RESULTS

Moiré-Fringe Method

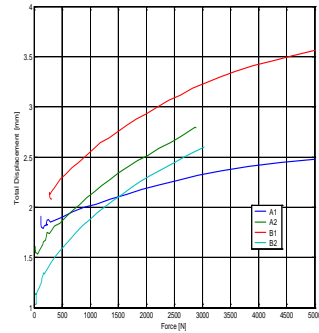


Fig. 7
The loading schemas.

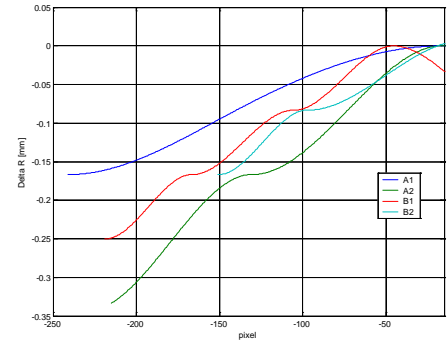
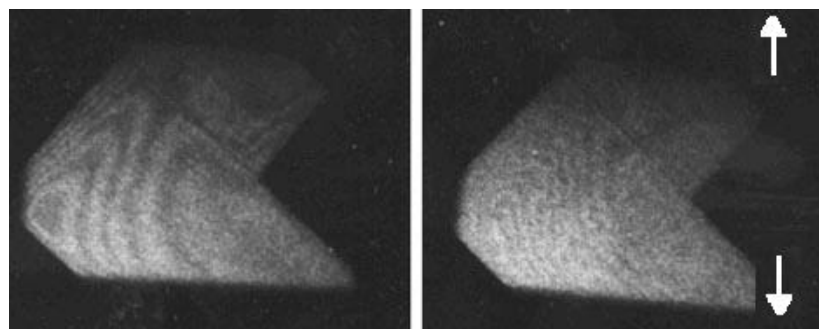
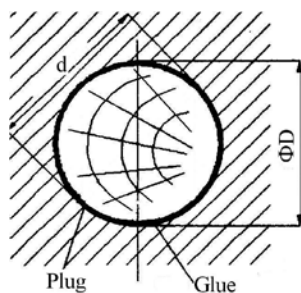


Fig. 8
The total diametrical displacements.

Fig. 9
The displacements offered by Moiré fringes evaluation.

The presented testing device was used in the case of some beech wood specimens (obtained after **L-R** anatomical main directions) with 80mm diameter and 8mm thickness. The relative positioning of the grids are presented in Fig. 7, where the dotted lines offer the fibre direction and **MG** represents the Object Grid's direction. The applied force's direction presented 0°, 30°, 60°, respectively 90° related to the fibre direction. The grid line density was 12 lines/mm. In accordance with the theory of the orthotropic materials (in our case: the wood materials) (Szalai 1995, 2001), the maximal value of the stiffness and the strength are observed along the fibre direction and together with the growing of the angle between the applied force direction and the fibre orientation, these values will decrease. Fig. 8 shows the comparative results of these diametrical displacements, obtained by means of the described electric strain gauge devices. These results are in accordance with the above mentioned theory. Fig. 9 offers the comparative results of calculus's, by means of the own-developed fringe evaluation method. These results show the vertical diametrical contraction, more exactly ΔR values, which means the upper radius modification; the numbering of the pixels starts from the centre of the disks. One can observe a good accordance with the measured results, but one have to specify, that the grids were fixed only on a circle with 70mm diameter. From this reason, the total displacements obtained in this second case (by evaluation of the moiré fringes) are smaller.

Holographic Interferometry



a.
Fig. 10
The wood joint stiffness evaluation.

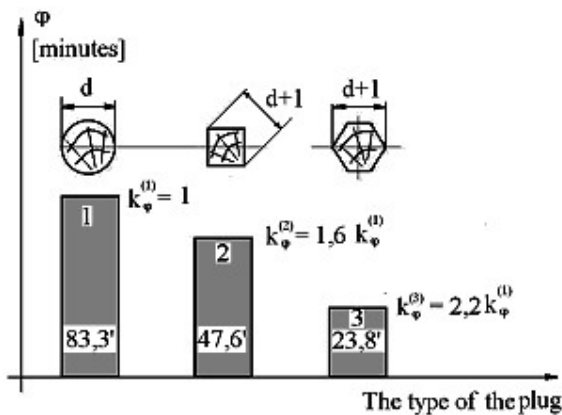


Fig. 11

The comparative results of stiffness, taking as reference the classical cylindrical plugs.

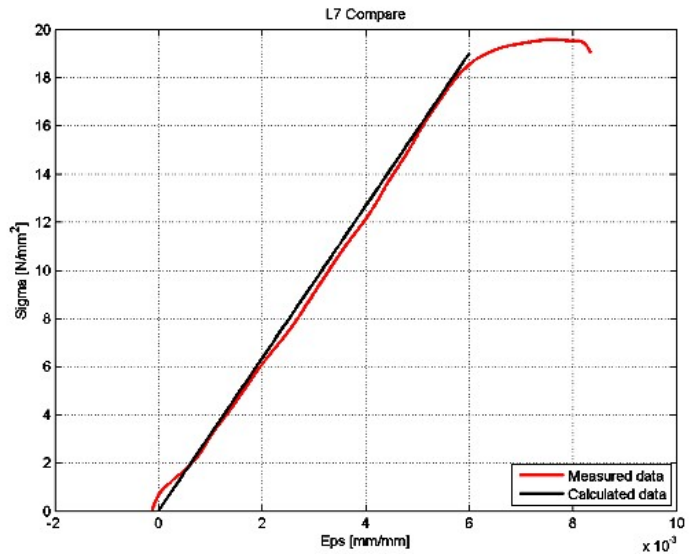


Fig. 12

The compared values for the third specimen.

The authors proposed the comparative stiffness evaluation of different wood-joints, using Holographic Interferometry, in order to establish the optimal shape of the used plugs as joining elements. It is well-known fact that the usual shape of plugs at gluing zone is the circular section, but at present there are attempt to use plugs with square and hexagonal sections, too. These last solutions assure possibility to introduce more adhesive, thus increase the strength of joints. Was conceived an original holographic stand, presented in the reference (Száva *et al.* 2000). Using this stand, were performed some detailed researches for establishing the optimal shape of the plug section. Thus, was established the condition for a maximal angular stiffness of the joints: $d + (1...2)mm > D$, where d represents the diameter of the plug, and D - the foreseen hole in wood members. Fig. 10 shows as illustration for one type of joints: the holograms both for initial (Fig. 10a) and final states (Fig. 10b), corresponding to a maximal force $F = 1.44 N$. In accordance with Theory of Plane Holography were calculated the angular displacements $\varphi [rad]$, respectively the corresponding angular stiffness $k [N \cdot mm]$. Fig. 11 shows the results of these comparative results of the experimental investigations.

Video Image Correlation

In order to illustrate the usefulness and the efficiency of the VIC-3D system, the authors offer the preliminary results on establishing the Young moduli (E_1 , E_2) of the components (the early-, and late-wood parts) for a pine-wood (a widely used soft-wood material), based only on a simple compression test. Due to the fact, that this sort of wood is applied/used mainly for working-out of the cross-section along the Tangential-Radial main natural direction, in the experiments the specimens were manufactured along these main natural direction. In this case, the early-wood (#1) and late-wood (#2) parts are parallel-connected. One can states for a given specimen (marked k) the stress-strain states based on well-known relations from Strength of Materials:

$$\begin{cases} F_k = N_{k1} + N_{k2} ; \\ \Delta \ell_{k1} = \Delta \ell_{k2} = \Delta \ell , \end{cases} \quad (2)$$

from where, one can obtain the corresponding forces (N_{k1} , N_{k2}), respectively the relationship between the Young moduli, the component parts' areas, the applied force and the global, measured strain:

$$A_{k1} \cdot E_1 + A_{k2} \cdot E_2 = F_k / \varepsilon_k . \quad (3)$$

$\ell_{k,0} [mm]$ - the initial length of the specimen k ;

$A_{k,1}$, $A_{k,2}$ [mm^2] - the cross-sectional areas of the constitutive parts #1 and #2.

Similarly, for the second tested specimen m will result:

$$A_{m1} \cdot E_1 + A_{m2} \cdot E_2 = F_m / \varepsilon_m . \quad (4)$$

and from the system (3-4) one will obtain the requested unknowns E_1 and E_2 .

The third specimen, marked with g , serves to verify/validate the obtained values. This specimen has also the same dimensions but different ratio between the earlier and later wood parts (A_{g1}, A_{g2}). One can calculate for this specimen a so-called *equivalent Young modulus*

$$E_g = \frac{\sigma_g}{\varepsilon_g} = \frac{F_g}{A_g \cdot \varepsilon_g} = \frac{A_{g1} \cdot E_1 + A_{g2} \cdot E_2}{A_g} . \quad (5)$$

Using this E_g , became possible to predict the linear zone of the stress-strain curve $\sigma - \varepsilon$, and to compare it with the real, experimental-obtained, stress-strain curve (see Fig. 12). By measuring and calculus, were obtained the corresponding areas of the specimens: for $L8 \equiv k$: $A_1 = 364.86 mm^2$; $A_2 = 35.14 mm^2$;

for $L6 \equiv m$: $A_1 = 352.25 mm^2$; $A_2 = 47.75 mm^2$; for $L7 \equiv g$: $A_1 = 364.86 mm^2$; $A_2 = 35.14 mm^2$.

Was to draw-up the corresponding stress-strain curves, and finally the requested Young modulus, corresponding to the force magnitude [$2000N \div 8000N$]: $E_{1,average} = 2858.59 N / mm^2$,

$$E_{2,average} = 14486.36 N / mm^2 .$$

CONCLUSIONS

Based on the above-described results, one can conclude the followings:

- In principle, the accuracy of the Moiré Fringe Methods depends strongly from the pitch (p) of the grid (s);
- Even the Moiré Fringe Methods has a relative low accuracy, in several cases of the wood-based materials it can be applied as relative cheap preliminary method;
- The Holographic Interferometry is the best-accuracy method, but it remains only a lab-method, due to its very sever requirements on vibration insulations, respectively the maximal displacements (lower than $\lambda / 2$);
- Up to this moment, the VIC-3D fulfils in the best manner the proposed investigations' requirements, due to its facilities, especially for the orthotropic and anisotropic materials and structures.

The above-presented results represent, at least at Romanian level, some original approaches and the described stands are fully originals.

ACKNOWLEDGMENTS

The authors express their gratitude and their special thanks to ISI-SYS GmbH, Germany (www.isi-sys.com), the system's producer, and Correlation Solution Company, USA (www.correlatedsolutions.com), the software producer, for their help, offering us (for limited period) the use of the VIC-3D (2009) program.

REFERENCES

- Bucur V (2006) Acoustics of wood. Springer Verlag, Berlin
- Gálfi BP, Száva I, Kakucs A, Harangus K (2010) Experimental investigation combined with analytical calculus for orthotropic materials' mechanical behaviours evaluation, Ovidius University Annuals, Scientific Journal, Mechanical Engineering Series, Vol. XII, TOM 1, 2010, Ovidius University Press, ISSN 1224-1776, pp. 187-190
- Hering S, Keunecke D, Niemz P (2012) "Moisture-dependent orthotropic elasticity of beech wood," Wood Sci. Technol. 46:927-938
- Hering S, Niemz P (2012) "Moisture-dependent, pure viscoelastic creep of European beech wood in longitudinal direction," Eur. J. Wood Wood Prod. 70(5):667-670
- Jones R, Wykes C (1983) Holographic and Speckle Interferometry, A discussion of the theory, practice and

application of the techniques. Cambridge University Press, Cambridge

Niemz P, Schreiber J, Naumann J, Stockmann M (2007) Experimentelle Ermittlung der Dehnungen im Probenquerschnitt bei Biegebelastung von Holzpartikelwerkstoffen, Holz. Roh. Werkst. Vol. 65:459-46

Niemz P, Mannes D (2012) Non-destructive testing of wood and wood-based materials, Journal of Cultural Heritage 135:26-34, Elsevier

Ozyhar T, Hering S, Niemz P (2012) Moisture-dependent elastic and strength anisotropy of European beech wood in tension, Journal of Materials Science, Vol. 47(2):6141-6150

Ozyhar T, Jüstrich S, Niemz P (2012) Tensile, compressive and bending properties of European beech wood at high moisture levels, Annals of Warsaw University of Life Science –SGGW-, Forestry and Wood Technology, No. 79:135-142

Ozyhar T, Hering S, Niemz P (2013) Viscoelastic characterisation of wood: Time dependence of the orthotropic compliance in tension and compression, Journal of Rheology, Vol. 57(2):699-717

Ozyhar T, Hering S, Niemz P (2013) Moisture-dependent orthotropic tension-compression asymmetry of wood, Holzforschung, Vol. 67(4):395-404

Ozyhar T, Hering S, Sanabria SJ, Niemz P (2013) Determining moisture-dependent elastic characteristics of beech wood by means of ultrasonic waves, Wood Science and Technology, Journal of the International Academy of Wood Science, Vol. 47(2):329-341

Szalai J (2001) Mérnöki faszervezetek. II. kötet. Mezőgazdasági Szaktudás kiadó. Budapest, pp. 143 -259

Szalai J (1995) A faanyag és faalapú anyagok anizotrop rugalmasság- és szilárdságtana, Vol. I., Hillebrand Nyomda KFT. Sopron

Száva I, Curtu I, Ciofoaia V, Botis M, Dogaru FI (2000) The experimental and theoretical study of optima shape at plugs for jointing elements in wood-based materials. Proc. of the 12th International Symposium on Nondestructive Testing of Wood (Wood NDT 2000), pp. 7-13

Száva I (2005) Holographic Interferometry and Moiré Fringes methods as efficient NDT methods in hardwood materials research (Material Characteristics, Optimisation of Shape etc), "Hardwood Research and Utilisation in Europe, New Challenges", University of West Hungary, Sopron, Hungary, Proceeding of Conference, pp. 9-19

Száva I, Gálfi BP, Szalai J, Kakucs A, Sárosi P (2007) Moiré Fringes Method used in Materials Characteristics Evaluation for Wood-based Materials, The 3rd Conference on Hardwood Research and Utilisation in Europe, University of West Hungary, Sopron, Proceedings of the Conference, pp. 7-16

Sutton AM, Ortu JJ, Schreier WH (2010) Image Correlation for Shape, Motion and Deformation Measurements, Springer Verlag

Theocaris SP (1969) Moiré fringes in Strain Analysis. Pergamon Press, Oxford, London

Valla A, Konnerth J, Keunecke D, Niemz P, Müller U, Gindl W (2010) Comparison of two optical methods for contactless, full field and highly sensitive in-plane deformation measurements using the example of plywood, Wood Sci. Technol. On-line published, Springer

VIC-3D (2010) Reference Manual. Correlated Solutions & ISI-Sys GmbH, USA, Kassel, Germany